

Water-Soluble Mixed-Ligand Ruthenium(II) and Osmium(II) Arene Complexes with High Antiproliferative Activity

Raffael Schuecker, Roland O. John, Michael A. Jakupec, Vladimir B. Arion,* and Bernhard K. Keppler*

Institute of Inorganic Chemistry, University of Vienna, Währinger Str. 42, A-1090 Vienna, Austria

Received August 12, 2008

The synthesis of ruthenium(II) and osmium(II) arene complexes of the general formula $[(\eta^6\text{-}p\text{-cymene})\text{M}(\text{oxine})(\text{Hazole})]\text{X}$, where M = Ru, Os; oxine = deprotonated 8-hydroxyquinoline, and Hazole = azole heterocycle, i.e., pyrazole (Hpz), indazole (Hind), imidazole (Him), benzimidazole (Hbzim), or 5,6-dimethylbenzimidazole (Hdmbzim); X = CF_3SO_3^- , PF_6^- , or Cl^- , combining ligands involved in metal-based complexes that are currently in clinical development, is reported. The compounds have been comprehensively characterized by elemental analysis, ESI mass spectrometry, spectroscopy (IR, UV–vis, NMR), and X-ray crystallography. The synthesis of these complexes was performed in order to achieve a balance between aqueous solubility and lipophilicity. The ruthenium(II) and osmium(II) compounds exhibit excellent cytotoxic effects in the tumor cell lines CH1 and SW480, with IC_{50} values ranging from 3.3 to 9.4 μM . As expected, the compounds are water soluble and show no evidence of hydrolysis or ligand exchange in aqueous media, which makes them noteworthy candidates for further development. The complexes $[(\eta^6\text{-}p\text{-cymene})\text{M}(\text{oxine})(\text{Hazole})]^+$ do not react with DNA purine bases, even if the latter are present in excess. However, the complex $[(\eta^6\text{-}p\text{-cymene})\text{Os}(\text{oxine})\text{Cl}]$ reacts with 9-methyladenine (meade) to form $[(\eta^6\text{-}p\text{-cymene})\text{Os}(\text{oxine})\text{meade}]^+$, which was isolated and characterized by X-ray diffraction as a hexafluorophosphate salt.

Introduction

Coordination chemistry offers great opportunities for the development of metal-containing anticancer agents.¹ Besides the platinum compounds used routinely in the clinic,^{2,3} two ruthenium-based complexes, namely, $(\text{H}_2\text{ind})[\text{trans-RuCl}_4\text{-(Hind)}_2]$ (KP1019)⁴ and $(\text{H}_2\text{im})[\text{trans-RuCl}_4\text{-(Him)(DMSO)}]$ (NAMI-A),⁵ are currently in clinical studies. In addition, the gallium complex $\text{Ga}(\text{oxine})_3$ (KP46), where oxine = deprotonated 8-hydroxyquinoline, showed promising results in a phase I clinical trial.⁶ Organometallic compounds of “three-leg piano-stool geometry” of the general formula $[(\eta^6\text{-arene})\text{M}(\text{XY})(\text{Z})]$ (where arene is biphenyl, benzene, or *p*-cymene; M = Ru, Os; XY is a bidentate chelating ligand; and Z a monodentate ligand) and $[(\eta^6\text{-arene})\text{Ru}(\text{PTA})\text{Cl}_2]$ complexes, where PTA = 1,3,5-triaza-7-phosphaadamantane,⁷ have also gained much attention

as promising antitumor agents.⁸ Recent studies have shown that the aqueous behavior of $[(\eta^6\text{-arene})\text{M}(\text{XY})(\text{Z})]$ compounds is highly dependent on the identity of the ligands and especially of the chelating one.^{9,10}

Our idea for the design of novel metal-based compounds with anticancer activity explored in the present study is based on a combination of typical features of the above-mentioned compounds in order to achieve both efficacy and a balance of aqueous solubility and lipophilicity. We found the half-sandwich piano-stool geometry with Ru(II) and Os(II) as metal ions and *p*-cymene as the arene ligand well suited for further development, because this coordination mode stabilizes the metal ion in its low oxidation state. As suggested for various Ru(III) complexes including KP1019, the reduced Ru(II) complex¹¹ might be the biologically relevant species. Thus, KP1019 acts as a prodrug, being reduced in tumor tissue to its active species. The use of a half-sandwich piano-stool complex enables the synthesis of air-stable Ru(II) and Os(II) complexes. The choice of the remaining components seems to be crucial. If only

* To whom correspondence should be addressed. E-mail: vladimir.arion@univie.ac.at (V.B.A.), bernhard.keppler@univie.ac.at (B.K.K.). Fax: +43 1 4277 52630 (V.B.A.), +43 1 4277 52680 (B.K.K.).

(1) Guo, Z.; Sadler, P. J. *Angew. Chem., Int. Ed.* **1999**, *38*, 1512–1531.

(2) Lippert, B., Ed. *Cisplatin. Chemistry and Biochemistry of a Leading Anticancer Drug*; VHCA & Wiley-VCH: Zurich, 1999.

(3) Galanski, M.; Arion, V. B.; Jakupec, M. A.; Keppler, B. K. *Curr. Pharm. Des.* **2003**, *9*, 2078–2089.

(4) Hartinger, C. G.; Zorbas-Seifried, S.; Jakupec, M. A.; Kynast, B.; Zorbas, H.; Keppler, B. K. *J. Inorg. Biochem.* **2006**, *100*, 891–904.

(5) Alessio, E.; Mestroni, G.; Bergamo, B.; Sava, G. *Curr. Top. Med. Chem.* **2004**, *4*, 1525–1535.

(6) Collery, P.; Jakupec, M. A.; Kynast, B.; Keppler, B. K. *Met. Ions Biol. Med.* **2006**, *9*, 521–524.

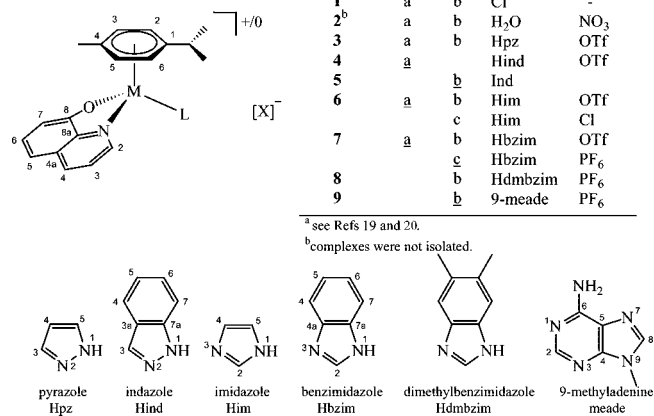
(7) (a) Ang, W. H.; Dyson, P. J. *Eur. J. Inorg. Chem.* **2006**, *20*, 4003–4018. (b) Ang, W. H.; Daldini, E.; Scopelliti, R.; Juillerat-Jeannerat, L.; Dyson, P. J. *Inorg. Chem.* **2006**, *45*, 9006–9013. (c) Gossens, C.; Dorcier, A.; Dyson, P. J.; Rothlisberger, U. *Organometallics* **2007**, *26*, 3965–3975. (d) Dyson, P. J.; Sava, G. *Dalton Trans.* **2006**, 1929–1933.

(8) (a) Aird, R. E.; Cummings, J.; Ritchie, A. A.; Muir, M.; Morris, R. E.; Chen, H.; Sadler, P. J. *Br. J. Cancer* **2002**, *86*, 1652–1657. (b) Melchart, M.; Sadler, P. J. *Bioorganometallics* **2006**, 39–64. (c) Morris, R. E.; Aird, R. E.; Murdoch, P. D. S.; Chen, H.; Cummings, J.; Hughes, N. D.; Parsons, S.; Parkin, A.; Boyd, G.; Jodrell, D. I.; Sadler, P. J. *J. Med. Chem.* **2001**, *44*, 3616–3621. (d) Sclaro, C.; Bergamo, A.; Brescacin, L.; Delfino, R.; Coccietto, M.; Laurency, G.; Geldbach, T. J.; Sava, G.; Dyson, P. J. *J. Med. Chem.* **2005**, *48*, 4161–4171. (e) Dorcier, A.; Ang, W. H.; Bolano, S.; Gonsalvi, L.; Juillerat-Jeannerat, L.; Laurency, G.; Peruzzini, M.; Phillips, A. D.; Zanobini, F.; Dyson, P. J. *Organometallics* **2006**, *25*, 4090–4096.

(9) Wang, F.; Chen, H.; Parsons, S.; Oswald, I. D. H.; Davidson, J. E.; Sadler, P. J. *Chem.–Eur. J.* **2003**, *9*, 5810–5820.

(10) Chen, H.; Parkinson, J. A.; Novakova, O.; Bella, J.; Wang, F.; Dawson, A.; Gould, R.; Parsons, S.; Brabec, V.; Sadler, P. J. *Proc. Natl. Acad. Sci. U.S.A.* **2003**, *100*, 14623–14628.

(11) Clarke, M. J. *Coord. Chem. Rev.* **2003**, *236*, 209–233.

Chart 1. Compounds Reported in This Work^a


Compound	Ru	Os	L	X
1 ^a	a	b	Cl	-
2 ^b	a	b	H ₂ O	NO ₃
3	a	b	Hpz	OTf
4	a	b	Hind	OTf
5	b	b	Him	OTf
6	a	b	Him	Cl
7	a	b	Hbzim	OTf
8	c	b	Hdbzim	PF ₆
9	b	b	9-meade	PF ₆

^a see Refs 19 and 20.
^b complexes were not isolated.

^a Underlined complexes have been characterized by X-ray crystallography; atom labeling was introduced for assignment of resonances in NMR spectra.

monodentate ligands are employed, this can generate hydrolysis products that make administration difficult.^{12,13} Taking into account the composition of KP46, we chose 8-hydroxyquinoline as an *N,O*-chelating ligand in order to prevent unwanted hydrolysis reactions. The sixth coordination site is occupied by an azole heterocycle, such as those acting as a ligand in KPI019 or NAMI-A. We expected to generate complexes capable of penetrating the cell membrane readily, at the same time possessing sufficient water solubility. To this end, azole heterocycles differing in their aqueous solubility and lipophilicity (Chart 1) were chosen. Since Os(II) as the heavier congener of Ru(II) is expected to be kinetically more inert,^{14,17–21} it was obvious to compare the hydrolytic behavior and the cytotoxicity of Ru(II) and Os(II) complexes with identical sets of ligands.

Herein, we report on the synthesis of Ru(II) and Os(II) arene complexes of the general formula $[(\eta^6\text{-}p\text{-cymene})\text{M}(\text{oxine})\text{-(Hazole)}]\text{X}$ (where M = Ru, Os; oxine = deprotonated 8-hydroxyquinoline; Hazole = azole heterocycle, i.e., indazole, pyrazole, imidazole, benzimidazole, or 5,6-dimethylbenzimidazole; X = $[\text{PF}_6]^-$ or OTf^-), their spectroscopic and X-ray

diffraction characterization, hydrolytic stability, reactivity toward purine bases, and high antiproliferative activity in two human cancer cell lines *in vitro*.

Experimental Section

Starting Materials. All chemicals were standard reagent grade and used without further purification. The solvents were purified according to standard procedures.¹⁵ RuCl₃ and OsO₄ were purchased from Johnson Matthey. AgCF₃SO₃, 8-hydroxyquinoline, and the azole compounds (imidazole, benzimidazole, 5,6-dimethylbenzimidazole, pyrazole, and indazole) were purchased from Fluka. The deuterated solvents were from Aldrich and dried over 4 Å molecular sieves. The precursors $[(\eta^6\text{-}p\text{-cymene})\text{RuCl}_2]$,¹⁶ $[(\eta^6\text{-}p\text{-cymene})\text{OsCl}_2]$,¹⁷ K(oxine),¹⁸ $[(\eta^6\text{-}p\text{-cymene})(\text{oxine})\text{RuCl}]$,¹⁹ and $[(\eta^6\text{-}p\text{-cymene})(\text{oxine})\text{OsCl}]$ ²⁰ were prepared according to literature protocols.

Preparation of Aqueous Solutions of $[(\eta^6\text{-}p\text{-cymene})\text{Ru}(\text{oxine})(\text{H}_2\text{O})\text{NO}_3]$ (2a**) and $[(\eta^6\text{-}p\text{-cymene})\text{Os}(\text{oxine})(\text{H}_2\text{O})\text{NO}_3]$ (**2b**) for a Cytotoxicity Assay.** In an Eppendorf tube to $[(\eta^6\text{-}p\text{-cymene})(\text{oxine})\text{RuCl}]$ (**1a**) (20 μM) or $[(\eta^6\text{-}p\text{-cymene})(\text{oxine})\text{OsCl}]$ (**1b**) (20 μM) were added AgNO₃ (20 μM) and H₂O (1 mL). The tubes were treated in an ultrasound bath for 5 min and then centrifuged at 14000 rpm for 5 min. The clear solutions were used for cytotoxicity tests.

Synthesis of Metal Complexes. All manipulations were performed under argon by using standard Schlenk techniques.

Complexes with Azole Ligands, General Procedure A. A suspension of **1a** (100 mg, 0.24 mmol) and silver triflate (65 mg, 0.25 mmol) in THF (5 mL) was stirred at room temperature for 2 h, and then the azole ligand (0.24 mmol) was added. After stirring the reaction mixture for 2 h, the solution was transferred to a centrifuge tube and centrifuged at 4000 rpm for 5 min. The supernatant was transferred into a Schlenk tube, and the solvent was removed under reduced pressure. The residue was dissolved in dichloromethane (2 mL). Addition of diethyl ether (15 mL) resulted in precipitation of a yellow product, which was filtered off, washed with diethyl ether (2 × 5 mL), and dried *in vacuo*.

Complexes with Azole Ligands, General Procedure B. To a suspension of **1b** (250 mg, 0.5 mmol) and silver triflate (128 mg, 0.5 mmol) in methanol (5 mL), stirred at ambient temperature for 30 min, was added the azole ligand (0.5 mmol), and stirring continued for 30 min. The solvent was removed under reduced pressure and the remaining solid suspended in dichloromethane (5 mL). Filtration of the suspension over Celite and concentration of the filtrate to 0.5 mL, followed by addition of diethyl ether (5 mL), gave rise to a yellow precipitate. The mixture was stirred for 18 h, and the product was filtered off, washed with diethyl ether (2 × 2 mL), and dried *in vacuo*.

$[(\eta^6\text{-}p\text{-cymene})\text{Ru}(\text{oxine})(\text{Hpz})]\text{CF}_3\text{SO}_3$ (3a**).** General Procedure A. Yield: 96 mg, 67% of a bright yellow powder. Anal. Calcd for C₂₃H₂₄F₃N₃O₄RuS (*M*_r 596.16): C, 46.31; H, 4.06; N, 7.04; S, 5.37. Found: C, 46.14; H, 4.04; N, 6.94; S, 5.21. ESI-MS: positive, *m/z* 447 $[(\eta^6\text{-}p\text{-cymene})\text{Ru}(\text{oxine})(\text{Hpz})]^+$, 380 $[(\eta^6\text{-}p\text{-cymene})\text{Ru}(\text{oxine})]^{2+}$; negative, *m/z* 149 $[\text{CF}_3\text{SO}_3]^-$. Solubility in water: 3.4 mM. IR spectrum (selected bands, KBr, ν_{max} , cm⁻¹): 523, 631, 749, 799, 1033, 1054, 1109, 1167, 1251, 1324, 1376, 1468, 1496, 1566, 2965, 3056, 3138. UV-vis spectrum [methanol, λ_{max} , nm (ϵ , M⁻¹ cm⁻¹): 263 (19 330), 240 (17 130) 420 (4100), 321 (3090), 335 (3050). ¹H NMR [400.13 MHz, CDCl₃, δ_{H} , ppm]: 13.00 [bs (broad singlet), 1H, pyrazole^{NH1}], 9.60 (d, ³*J*_{HH} = 4.5 Hz, 1H, hc²), 8.07 (d, ³*J*_{HH} = 8.5 Hz, 1H, hc⁴), 7.56 (d, ³*J*_{HH} = 2.0 Hz, 1H, pyrazole^{3/5}), 7.48 (q, ³*J*_{HH} = 4.5 Hz, 1H, hc³), 7.39 (d, ³*J*_{HH} = 2.0 Hz, 1H, pyrazole^{3/5}), 7.32 (t, ³*J*_{HH} = 8.0 Hz, 1H, hc⁶), 7.03 (d, ³*J*_{HH} = 8.0 Hz, 1H, hc⁷), 6.85 (d, ³*J*_{HH} = 8.0 Hz, 1H, hc⁵), 6.12 (m, 1H, pyrazole⁴), 6.04 [d, ³*J*_{HH} = 6.0 Hz, 1H, cy (cymene)], 5.83 (t, ³*J*_{HH} = 7.0 Hz, 2H, cy), 5.79 (d, ³*J*_{HH} = 6.0 Hz, 1H, cy), 2.39 (m, 1H, CHMe₂), 1.87 (s, 3H, CH₃), 1.11 (d, ³*J*_{HH} = 6.5 Hz, 3H, CHMe₂), 0.89 (d, ³*J*_{HH} =

(12) Yan, Y. K.; Melchart, M.; Habtemariam, A.; Sadler, P. J. *Chem. Commun.* **2005**, 38, 4764–4776.

(13) Peacock, A. F. A.; Melchart, M.; Deeth, R. J.; Habtemariam, A.; Parsons, S.; Sadler, P. J. *Chem.–Eur. J.* **2007**, 13, 2601–2613.

(14) (a) Shriver, D. F.; Atkins, P. W. *Inorganic Chemistry*, 3rd ed.; Oxford University Press: Oxford, 1999; p 245. (b) Griffith, W. P. In *Comprehensive Coordination Chemistry*, Vol. 4; Pergamon: Oxford, 1987; pp 519–633. (c) Ashby, M. T.; Alguindigue, S. S.; Khan, M. A. *Organometallics* **2000**, 19, 547–552. (d) George, R.; Andersen, J.-A. M.; Moss, J. R. *J. Organomet. Chem.* **1995**, 505, 131–133. (e) Halpern, J.; Cai, L.; Desrosiers, P. J.; Lin, Z. *J. Chem. Soc., Dalton Trans.* **1991**, 717–723.

(15) Armarego, W. L. *Purification of Laboratory Chemicals*; Elsevier Science: Zurich, 2003.

(16) Bennett, M. A.; Smith, A. K. *J. Chem. Soc., Dalton Trans.* **1974**, 233–241.

(17) Kiel, W. A.; Ball, R. G.; Graham, W. A. *J. Organomet. Chem.* **1990**, 383, 481–496.

(18) Sue, P.; Wetroff, G. *Bull. Soc. Chim.* **1935**, 2, 1002–1007.

(19) Gemel, C.; John, R.; Slugovic, C.; Mereiter, K.; Schmid, R.; Kirchner, K. *J. Chem. Soc., Dalton Trans.* **2000**, 2607–2612.

(20) Peacock, A. F. A.; Parsons, S.; Sadler, P. J. *J. Am. Chem. Soc.* **2007**, 129, 3348–3357.

(21) (a) Otwinowski, Z.; Minor, W. In *Methods in Enzymology*, Vol. 276 (*Macromolecular Crystallography*, part A); Carter, C. W., Jr., Sweet, R. M., Eds.; Academic Press: New York, 1997; pp 307–326. (b) SAINT-Plus, version 7.06a and APEX2; Bruker-Nonius AXS Inc.: Madison, WI, 2004.

7.0 Hz, 3H, CHMe₂). ¹³C{¹H} NMR [100.63 MHz, CDCl₃, δ_C, ppm]: 167.5 (C⁸), 152.2 (C²), 143.4 (C^{8a}), 137.8 (C⁴), 136.7 (pyrazole-C^{3/5}), 134.0 (pyrazole-C^{3/5}), 131.0 (C⁶), 130.1 (C^{4a}), 123.0 (C³), 114.8 (C⁷), 113.2 (C⁵), 105.2 (pyrazole-C⁴), 92.4 (cy-C¹), 91.7 (cy-C⁴), 75.6, 72.4, 72.1, 71.2 (cy-C^{2,3,5,6}), 30.6 (CHMe₂), 23.0, 22.1 (CHMe₂), 17.8 (Me).

[(η⁶-*p*-cymene)Os(oxine)(Hpz)]CF₃SO₃ (**3b**). General Procedure B. Yield: 207 mg, 61% of a yellow powder. Anal. Calcd for C₂₃H₂₄F₃N₃O₄OsS (M_r 685.74): C, 40.28; H, 3.53; N, 6.13; S, 4.68. Found: C, 40.04; H, 3.42; N, 6.17; S, 4.72. ESI-MS: positive, *m/z* 538 [(η⁶-*p*-cymene)Os(oxine)(Hpz)]⁺, 470 [(η⁶-*p*-cymene)Os(oxine)]⁺; negative, *m/z* 149 [CF₃SO₃]⁻. Solubility in water: 1.2 mM. IR spectrum (selected bands, KBr, ν_{max}, cm⁻¹): 520, 636, 760, 822, 1031, 1051, 1112, 1164, 1247, 1289, 1323, 1374, 1466, 1500, 1575, 2966, 3058, 3141. UV-vis spectrum [water, λ_{max}, nm (ε, M⁻¹ cm⁻¹): 230 (20 430), 261 (19 370), 418 (4220), 324 (3190), 336 (3070).

[(η⁶-*p*-cymene)Ru(oxine)(Hind)]CF₃SO₃·CH₂Cl₂ (**4a**·CH₂Cl₂). General Procedure A. Purification by crystallization from dichloromethane/diethyl ether gave bright orange crystals of X-ray diffraction quality. Yield: 114 mg, 65%. Anal. Calcd for C₂₇H₂₆F₃N₃O₄RuS·CH₂Cl₂ (M_r 731.58): C, 45.97; H, 3.86; N, 5.74; S, 4.38. Found: C, 46.04; H, 3.87; N, 5.79; S, 4.39. ESI-MS: positive, *m/z* 646 [(η⁶-*p*-cymene)Ru(oxine)(Hind)]⁺, 380 [(η⁶-*p*-cymene)Ru(oxine)]⁺; negative, *m/z* 149 [CF₃SO₃]⁻. IR spectrum (selected bands, KBr, ν_{max}, cm⁻¹): 519, 639, 749, 823, 1031, 1111, 1170, 1285, 1321, 1375, 1467, 1500, 1574, 2972, 3073, 3225. UV-vis spectrum [methanol, λ_{max}, nm (ε, M⁻¹ cm⁻¹): 265 (21 440), 230 (20 040), 408 (4760), 320 (3370), 334 (3150). ¹H NMR [400.13 MHz, CDCl₃, δ_H, ppm]: 12.99 (bs, 1H, imidazole^{NH}), 9.58 (d, ³J_{HH} = 4.0 Hz, 1H, hc²), 8.05 (d, ³J_{HH} = 8.0 Hz, 1H, hc⁴), 7.90 (s, 1H, indazole³), 7.64 (d, ³J_{HH} = 8.5, 1H, indazole⁴), 7.48 (m, 2H, hc³, indazole⁷), 7.34 (m, 2H, hc⁶, indazole⁶), 7.07 (t, 2H, hc⁷, indazole⁵), 6.83 (d, ³J_{HH} = 8.0 Hz, 1H, hc⁵), 6.12 (d, ³J_{HH} = 6.0 Hz, 1H, cy), 5.90 (m, 3H, cy), 2.39 (m, ³J_{HH} = 6.8 Hz, 1H, CHMe₂), 1.87 (s, 3H, CH₃), 1.12 (d, ³J_{HH} = 7.0 Hz, 3H, CHMe₂), 0.88 (d, ³J_{HH} = 6.5 Hz, 3H, CHMe₂). ¹³C{¹H} NMR [100.63 MHz, CDCl₃, δ_C, ppm]: 167.8 (C⁸), 152.2 (C²), 142.6 (C^{8a}), 138.8 (C⁴), 135.5 (indazole-C³), 130.4 (C⁶), 130.3 (C^{4a}), 129.0 (indazole-C⁶), 123.5 (C³), 122.5 (indazole-C⁵), 122.1 (indazole-C^{3a}), 120.3 (indazole-C⁷), 118.1 (indazole-C^{7a}), 115.1 (C⁷), 112.6 (C⁵), 111.5 (indazole-C⁴), 104.4 (cy-C¹), 101.6 (cy-C⁴), 85.5, 85.4, 83.1, 82.9 (cy-C^{2,3,5,6}), 31.5 (CHMe₂), 23.1, 21.9 (CHMe₂) 18.6 (Me).

[(η⁶-*p*-cymene)Os(oxine)(ind)] (**5b**). A suspension of **1b** (100 mg, 0.2 mmol) and Ag₂CO₃ (28 mg, 0.1 mmol) in methanol (10 mL) was stirred for 2 h at room temperature. Then indazole (24 mg, 0.2 mmol) was added, and the mixture was stirred again for 2 h. The resulting white solid was filtered off, and half of the solvent was removed by rotary evaporation under reduced pressure. The solution was left to stand at 4 °C overnight. The crystals obtained were washed with diethyl ether (10 mL), recrystallized from acetonitrile, and dried *in vacuo*. Yield: 50 mg, 43% of a yellow powder. Anal. Calcd for C₂₆H₂₅N₃O₄Os (M_r 585.73): C, 53.31; H, 4.30; N, 7.17. Found: C, 53.21; H, 4.34; N, 7.17. ESI-MS: positive, *m/z* 587 [(η⁶-*p*-cymene)Os(oxine)(ind)]⁺, 470 [(η⁶-*p*-cymene)Os(oxine)]⁺. IR spectrum (selected bands, KBr, ν_{max}, cm⁻¹): 524, 750, 778, 818, 1064, 1111, 1192, 1322, 1374, 1466, 1499, 1570, 2957, 3014, 3044. UV-vis spectrum [methanol, λ_{max}, nm (ε, M⁻¹ cm⁻¹): 265 (23 400), 296 (9570), 304 (8420), 432 (3840), 342 (3480). ¹H NMR [400.13 MHz, CDCl₃, δ_H, ppm]: 9.05 (d, ³J_{HH} = 4.8 Hz, 1H, hc²), 7.79 (d, ³J_{HH} = 8.3 Hz, 1H, hc⁴), 7.66 (s, 1H, indazole³), 7.61 (d, ³J_{HH} = 8.6 Hz, 1H, indazole⁴), 7.43 (d, ³J_{HH} = 8.1 Hz, 1H, indazole⁷), 7.31 (m, 1H, hc⁶), 7.08 (d, ³J_{HH} = 7.9 Hz, 1H, hc⁷), 6.95 (m, 2H, hc³, indazole⁶), 6.73 (m, 2H, hc⁵, indazole⁵), 5.99 (d, ³J_{HH} = 5.6 Hz, 1H, cy), 5.95 (d, ³J_{HH} = 5.4 Hz, 1H, cy), 5.78 (m, 2H, cy), 2.38 (m, 1H, CHMe₂), 1.91 (s, 3H, Me), 1.07 (d, ³J_{HH} = 6.9 Hz, 3H, CHMe₂), 0.93 (d, ³J_{HH} = 6.9 Hz, 3H, CHMe₂). ¹³C{¹H}

NMR [100.63 MHz, CDCl₃, δ_C, ppm]: 170.4 (C⁸), 151.7 (indazole-C^{3a}), 149.5 (C²), 144.8 (C^{8a}), 138.0 (C⁴), 130.5 (C⁶), 130.4 (C^{4a}), 128.2 (indazole-C³), 122.6 (indazole-C^{7a}), 122.3 (C³), 122.2 (indazole-C⁶), 119.6 (indazole-C⁷), 117.9 (indazole-C⁵), 115.8 (indazole-C⁴), 114.8 (C⁷), 112.2 (C⁵), 94.0 (cy-C¹), 93.6 (cy-C⁴), 77.4, 74.2, 72.9, 71.2 (cy-C^{2,3,5,6}), 31.6 (CHMe₂), 23.5, 22.9 (CHMe₂), 18.1 (Me). Single crystals of **5b**·3CH₃OH suitable for X-ray diffraction measurements were grown in methanol.

[(η⁶-*p*-cymene)Ru(oxine)(Him)]CF₃SO₃ (**6a**). General Procedure A. Yield: 98 mg, 68% of a pale yellow powder. Anal. Calcd for C₂₃H₂₄F₃N₃O₄RuS (M_r 596.16): C, 46.31; H, 4.06; N, 7.04; S, 5.37. Found: C, 45.90; H, 3.97; N, 6.95; S, 5.19. ESI-MS: positive, *m/z* 447 [(η⁶-*p*-cymene)Ru(oxine)(Him)]⁺, 380 [(η⁶-*p*-cymene)Ru(oxine)]⁺; negative, *m/z* 149 [CF₃SO₃]⁻. Solubility in water: 2.8 mM. IR spectrum (selected bands, KBr, ν_{max}, cm⁻¹): 414, 520, 637, 748, 787, 824, 906, 1029, 1166, 1270, 1318, 1382, 1467, 1501, 1577, 1926, 2694, 2969, 3109. UV-vis spectrum [methanol, λ_{max}, nm (ε, M⁻¹ cm⁻¹): 231 (20 430), 266 (19 640). ¹H NMR [400.13 MHz, CDCl₃, δ_H, ppm]: 11.41 (bs, 1H, imidazole^{NH}), 9.37 (d, ³J_{HH} = 4.5 Hz, 1H, hc²), 7.48 (m, 2H, hc⁴, imidazole²), 7.41 (dd, ³J_{HH} = 5.2 Hz, ⁴J_{HH} = 3.4 Hz, 1H, hc³), 7.29 (t, ³J_{HH} = 8.0 Hz, 1H, hc⁶), 6.98 (d, ³J_{HH} = 7.5 Hz, 1H, hc⁷), 6.90 (s, 1H, imidazole⁵), 6.83 (m, 2H, hc⁵, imidazole⁵), 5.90 (d, ³J_{HH} = 6.0 Hz, 1H, cy), 5.75 (d, ³J_{HH} = 5.5 Hz, 1H, cy), 5.65 (d, ³J_{HH} = 6.0 Hz, 1H, cy), 5.61 (d, ³J_{HH} = 5.5 Hz, 1H, cy), 2.45 (m, ³J_{HH} = 7.0 Hz, 1H, CHMe₂), 1.85 (s, 3H, CH₃), 1.07 (d, ³J_{HH} = 6.5 Hz, 3H, CHMe₂) 0.96 (d, ³J_{HH} = 7.0 Hz, 3H, CHMe₂). ¹³C{¹H} NMR [100.63 MHz, CDCl₃, δ_C, ppm]: 168.0 (C⁸), 151.0 (C²), 143.6 (C^{8a}), 138.5 (C⁴), 138.6 (imidazole-C²), 130.5 (C⁶), 130.2 (C^{4a}), 127.7 (imidazole-C⁴), 123.3 (C³), 118.2 (imidazole-C⁵), 115.0 (C⁷), 112.1 (C⁵), 103.5 (cy-C¹), 101.5 (cy-C⁴), 85.9, 84.7, 82.0, 81.5 (cy-C^{2,3,5,6}), 31.4 (CHMe₂), 22.9, 22.3 (CHMe₂) and 18.3 (Me). X-ray diffraction quality single crystals were obtained by slow diffusion of diethyl ether into a CH₂Cl₂ solution of **6a**.

[(η⁶-*p*-cymene)Os(oxine)(Him)]CF₃SO₃ (**6b**). General Procedure B. Yield: 211 mg, 62% of a yellow powder. Anal. Calcd for C₂₃H₂₄F₃N₃O₄OsS (M_r 685.74): C, 40.28; H, 3.53; N, 6.13; S, 4.68. Found: C, 40.03; H, 3.47; N, 6.04; S, 4.55. ESI-MS: positive, *m/z* 470 [(η⁶-*p*-cymene)Os(oxine)]⁺; negative, *m/z* 149 [CF₃SO₃]⁻. Solubility in water: 0.9 mM. IR spectrum (selected bands, KBr, ν_{max}, cm⁻¹): 520, 637, 749, 824, 1028, 1070, 1107, 1164, 1272, 1318, 1383, 1467, 1502, 1577, 2635, 2781, 2928, 2964, 3107. UV-vis spectrum [methanol, λ_{max}, nm (ε, M⁻¹ cm⁻¹): 233 (17 220), 261 (16 560), 421 (4260), 324 (3160), 338 (3030).

[(η⁶-*p*-cymene)Os(oxine)(Him)]Cl (**6c**). A mixture of **1b** (200 mg, 0.4 mmol) and imidazole (27 mg, 0.4 mmol) in methanol (3 mL) was stirred for 18 h at ambient temperature. The resulting clear solution was filtered over Celite and concentrated under reduced pressure to 0.5 mL. Addition of diethyl ether (5 mL) resulted in a brown-yellow oil, which solidified upon vigorous stirring for 5 h. The bright yellow solid was collected by filtration, washed with diethyl ether (2 × 2 mL), and dried *in vacuo*. Yield: 189 mg, 83% of yellow hygroscopic powder. Anal. Calcd for C₂₂H₂₄ClN₃O₄Os (M_r 572.13): C, 45.47; H, 4.34; N, 7.23. Found: C, 45.30; H, 4.08; N, 7.11. ESI-MS: positive, *m/z* 470 [(η⁶-*p*-cymene)Os(oxine)]⁺. Solubility in water: 52.3 mM. IR spectrum (selected bands, KBr, ν_{max}, cm⁻¹): 526, 753, 824, 1076, 1111, 1283, 1320, 1377, 1465, 1499, 1573, 2625, 2800, 2909. UV-vis spectrum [water, λ_{max}, nm (ε, M⁻¹ cm⁻¹): 232 (18 110), 261 (17 480), 422 (4410), 442 (3940), 325 (3320), 337 (3190).

[(η⁶-*p*-cymene)Ru(oxine)(Hbzim)]CF₃SO₃ (**7a**). General Procedure A. Yield: 116 mg, 75%. Anal. Calcd for C₂₇H₂₆F₃N₃O₄RuS (M_r 646.64): C, 50.15; H, 4.05; N, 6.50; S, 4.96. Found: C, 49.65; H, 3.95; N, 6.47; S, 4.79. ESI-MS: positive, *m/z* 647 [(η⁶-*p*-cymene)Ru(oxine)(Hbzim)]⁺, 380 [(η⁶-*p*-cymene)Ru(oxine)]⁺; negative, *m/z* 149 [CF₃SO₃]⁻. Solubility in water: 0.9 mM. IR spectrum (selected bands, KBr, ν_{max}, cm⁻¹): 521, 563, 640, 775, 837, 1112,

1264, 1285, 1322, 1379, 1431, 1504, 1576, 2965, 3061, 3109. UV-vis spectrum [water, λ_{max} , nm (ϵ , $\text{M}^{-1} \text{cm}^{-1}$): 232 (18 540), 266 (17 736) 428 (4520), 328 (3380), 346 (3210). ^1H NMR [400.13 MHz, CDCl_3 , δ_{H} , ppm]: 12.00 (bs, 1H, benzimidazole^{NH}), 9.62 (d, $^3J_{\text{HH}} = 4.5$ Hz, 1H, hc^2), 8.29 (s, 1H, benzimidazole²), 8.04 (d, $^3J_{\text{HH}} = 8.0$ Hz, 1H, benzimidazole^{4/7}), 7.96 (d, $^3J_{\text{HH}} = 8.5$ Hz, 1H, hc^4), 7.44 (m, 2H, hc^3 , benzimidazole^{4/7}), 7.29 (t, $^3J_{\text{HH}} = 7.8$, 1H, hc^6), 7.15 (m, 2H, hc^7 , benzimidazole^{5/6}), 6.89 (d, $^3J_{\text{HH}} = 7.5$ Hz, 1H, benzimidazole^{5/6}), 6.71 (d, $^3J_{\text{HH}} = 7.6$ Hz, 1H, hc^5), 6.08 (d, $^3J_{\text{HH}} = 6.0$ Hz, 1H, cy), 5.88 (d, $^3J_{\text{HH}} = 6.0$, 1H, cy), 5.71 (d, $^3J_{\text{HH}} = 6.0$ Hz, 1H, cy), 5.68 (d, $^3J_{\text{HH}} = 6.0$, 1H, cy), 2.48 (m, $^3J_{\text{HH}} = 7.0$ Hz, 1H, CHMe_2), 1.65 (s, 3H, CH_3), 1.03 (d, $^3J_{\text{HH}} = 7.0$ Hz, 3H, CHMe_2) 0.94 (d, $^3J_{\text{HH}} = 7.0$ Hz, 3H, CHMe_2). $^{13}\text{C}\{^1\text{H}\}$ NMR [100.63 MHz, CDCl_3 , δ_{C} , ppm]: 167.8 (C^8), 151.9 (C^2), 143.9 (C^{8a}), 143.3 (benzimidazole- C^2), 140.8 (benzimidazole- $\text{C}^{4a/7a}$), 138.7 (C^4), 132.9 (benzimidazole- $\text{C}^{4a/7a}$), 130.5 (benzimidazole- $\text{C}^{5/6}$), 130.3 (C^{4a}), 124.9 (C^7), 124.4 (C^6), 123.2 (C^3), 118.3 (benzimidazole- $\text{C}^{4/7}$), 115.0 (benzimidazole- $\text{C}^{5/6}$), 113.8 (benzimidazole- $\text{C}^{4/7}$), 112.0 (C^5), 102.7 (cy- C^1), 102.5 (cy- C^4), 85.9, 84.7, 82.0, 81.5 (cy- $\text{C}^{2,3,5,6}$), 31.4 (CHMe_2), 22.9, 22.3 (CHMe_2) and 18.3 (Me). Single crystals of $7\mathbf{a} \cdot 0.5(\text{C}_2\text{H}_5)_2\text{O}$ were grown by slow diffusion of diethyl ether into a CH_3OH solution of $7\mathbf{a}$.

[(η^6 -*p*-cymene)Os(oxine)(Hbzim)]CF₃SO₃ (7b**). General Procedure B. Yield: 251 mg, 69% of a yellow powder. Anal. Calcd for $\text{C}_{27}\text{H}_{26}\text{F}_3\text{N}_3\text{O}_4\text{OsS}$ (M_r 735.80): C, 44.07; H, 3.56; N, 5.71; S, 4.36. Found: C, 44.28; H, 3.48; N, 5.75; S, 4.27. ESI-MS: positive, m/z 586 [(η^6 -*p*-cymene)Os(oxine)(Hbzim)]⁺, 470 [(η^6 -*p*-cymene)Os(oxine)]⁺; negative, m/z 149 [CF₃SO₃]⁻. Solubility in water: 0.3 mM. IR spectrum (selected bands, KBr, ν_{max} , cm^{-1}): 521, 639, 755, 827, 1031, 1112, 1162, 1264, 1322, 1379, 1466, 1501, 1574, 2924, 2965, 3109. UV-vis spectrum [water, λ_{max} , nm (ϵ , $\text{M}^{-1} \text{cm}^{-1}$): 232 (21 740), 263 (20 490), 426 (4420), 325 (3170), 338 (3030).**

[(η^6 -*p*-cymene)Os(oxine)(Hbzim)]PF₆ (7c**). To a suspension of **1b** (200 mg, 0.4 mmol) in methanol (10 mL) was added dropwise a solution of silver hexafluorophosphate (100 mg, 0.4 mmol) in methanol (2 mL), and the mixture was stirred for 2 h at room temperature. Benzimidazole (47 mg, 0.4 mmol) was added, and the mixture was stirred for an additional 2 h. The resulting white solid was filtered off, and half of the solvent was removed by rotary evaporation under reduced pressure. The concentrated solution was left to stand at 4 °C overnight. The crystals obtained were filtered off, washed with diethyl ether (5 mL), recrystallized from acetonitrile, and dried *in vacuo*. Yield: 209 mg, 72% of brown-yellow crystals. Anal. Calcd for $\text{C}_{26}\text{H}_{26}\text{F}_6\text{N}_3\text{O}_3\text{OsP}$ (M_r 731.70): C, 42.68; H, 3.58; N, 5.74. Found: C, 42.74; H, 3.38; N, 5.83. ESI-MS: positive, m/z 470 [(η^6 -*p*-cymene)Os(oxine)]⁺; negative, m/z 145 [PF₆]⁻. IR spectrum (selected bands, KBr, ν_{max} , cm^{-1}): 523, 555, 636, 737, 776, 840, 1113, 1247, 1281, 1320, 1377, 1425, 1465, 1501, 1574, 2965, 3058, 3157, 3335. UV-vis spectrum [methanol, λ_{max} , nm (ϵ , $\text{M}^{-1} \text{cm}^{-1}$): 233 (21 670), 266 (21 090), 435 (4350), 329 (3340), 341 (3180). X-ray diffraction quality single crystals of $7\mathbf{c} \cdot 2\text{CH}_3\text{OH}$ were grown from a saturated solution of **7c** in methanol.**

[(η^6 -*p*-cymene)Os(oxine)(Hdmbzim)]PF₆ (8b**). To a suspension of **1b** (200 mg, 0.4 mmol) in methanol (10 mL) was added dropwise a solution of silver hexafluorophosphate (100 mg, 0.4 mmol) in methanol (2 mL), and the mixture was stirred for 2 h at room temperature. Then 5,6-dimethylbenzimidazole (58 mg, 0.4 mmol) in methanol (2 mL) was added, and the mixture was stirred for an additional 2 h. The resulting white solid was filtered off, and half of the solvent was removed by rotary evaporation under reduced pressure. The concentrated solution was allowed to stand at 4 °C overnight. The product formed was filtered off, washed with cooled diethyl ether (2 mL), and dried *in vacuo*. Yield: 251 mg, 83% of yellow-brown crystals. Anal. Calcd for $\text{C}_{28}\text{H}_{30}\text{F}_6\text{N}_3\text{O}_3\text{OsP}$ (M_r 759.75): C, 44.26; H, 3.98; N, 5.53. Found: C, 44.20; H, 3.69; N,**

5.49. ESI-MS: positive, m/z 616 [(η^6 -*p*-cymene)Os(oxine)(Hdmbzim)]⁺, 470 [(η^6 -*p*-cymene)Os(oxine)]⁺; negative, m/z 145 [PF₆]⁻. IR spectrum (selected bands, KBr, ν_{max} , cm^{-1}): 527, 557, 749, 778, 845, 1113, 1282, 1319, 1377, 1466, 1501, 1574, 2962, 3371. UV-vis spectrum [methanol, λ_{max} , nm (ϵ , $\text{M}^{-1} \text{cm}^{-1}$): 265 (21 930), 287 (11 190). ^1H NMR [400.13 MHz, CDCl_3 , δ_{H} , ppm]: 10.19 (bs, 1H), 9.41 (d, $^3J_{\text{HH}} = 5.0$ Hz, 1H), 8.09 (m, 2H), 7.76 (s, 1H), 7.55 (dd, $^3J_{\text{HH}} = 8.4$ Hz, $^3J_{\text{HH}} = 5.0$ Hz, 1H), 7.25 (t, $^3J_{\text{HH}} = 8.0$ Hz, 1H), 7.16 (s, 1H), 6.91 (d, $^3J_{\text{HH}} = 8.0$ Hz, 1H), 6.82 (d, $^3J_{\text{HH}} = 8.0$ Hz, 1H), 6.23 (d, $^3J_{\text{HH}} = 5.6$ Hz, 1H), 6.20 (d, $^3J_{\text{HH}} = 5.6$ Hz, 1H), 5.94 (d, $^3J_{\text{HH}} = 5.6$ Hz, 1H), 5.89 (d, $^3J_{\text{HH}} = 5.6$ Hz, 1H), 2.42 (m, 4H), 2.28 (s, 3H), 1.79 (s, 3H), 1.05 (d, $^3J_{\text{HH}} = 6.9$ Hz, 3H), 0.98 (d, $^3J_{\text{HH}} = 6.9$ Hz, 3H).

[(η^6 -*p*-cymene)Os(oxine)(meade)]PF₆ (9b**). A mixture of **1b** (100 mg, 0.2 mmol) and 9-methyladenine (30 mg, 0.2 mmol) in methanol (5 mL) was stirred for 1 h in the dark at ambient temperature. The resulting clear orange solution was filtered directly into a solution of NH_4PF_6 (652 mg, 4.0 mmol) in water (10 mL). The yellow solid formed was collected by filtration, washed with water, and dried to receive the crude product, which was purified by diffusion of diethyl ether into a saturated methanolic solution of the compound. Yield: 70 mg, 47% of yellow-brown crystals suitable for X-ray diffraction measurements. Anal. Calcd for $\text{C}_{25}\text{H}_{27}\text{F}_6\text{N}_6\text{O}_3\text{OsP}$ (M_r 752.13): C, 39.37; H, 3.57; N, 11.02. Found: C, 39.31; H, 3.56; N, 10.92. ESI-MS: positive, m/z 617 [(η^6 -*p*-cymene)Os(oxine)(meade)]⁺, 470 [(η^6 -*p*-cymene)Os(oxine)]⁺. IR spectrum (selected bands, KBr, ν_{max} , cm^{-1}): 3307, 3139, 1652, 1576, 1504, 1467, 1378, 1320, 1279, 1240, 1112, 836, 785, 750, 557. UV-vis spectrum [water, λ_{max} , nm (ϵ , $\text{M}^{-1} \text{cm}^{-1}$): 208 (50 580), 264 (29 380), 235 (24 260), 435 (4350), 324 (4200), 340 (3680). ^1H NMR [400.13 MHz, CDCl_3 , δ_{H} , ppm]: 9.60 (dd, $^3J_{\text{HH}} = 5.1$ Hz, $^4J_{\text{HH}} = 1.1$ Hz, 1H, hc^2), 9.03 (bs, 1H, meade⁶- NH_2), 8.33 (s, 1H, meade²), 8.31 (s, 1H, meade⁸), 8.23 (dd, $^3J_{\text{HH}} = 8.5$ Hz, $^4J_{\text{HH}} = 1.1$ Hz, 1H, hc^4), 7.72 (dd, $^3J_{\text{HH}} = 8.5$ Hz, $^3J_{\text{HH}} = 5.1$ Hz, 1H, hc^3), 7.39 (t, $^3J_{\text{HH}} = 7.9$ Hz, 1H, hc^6), 6.99 (m, 2H, hc^5 , hc^7), 6.27 (d, $^3J_{\text{HH}} = 5.6$ Hz, 1H, cy), 6.19 (d, $^3J_{\text{HH}} = 5.6$ Hz, 1H, cy), 6.01 (d, $^3J_{\text{HH}} = 5.6$ Hz, 1H, cy), 5.94 (d, $^3J_{\text{HH}} = 5.6$ Hz, 1H, cy), 5.60 (bs, 1H, meade⁶- NH_2), 3.80 (s, 3H, meade-Me), 2.42 (m, 1H, CHMe_2), 1.74 (s, 3H, Me), 1.06 (d, $^3J_{\text{HH}} = 6.9$ Hz, 3H, CHMe_2), 0.91 (d, $^3J_{\text{HH}} = 6.9$ Hz, 3H, CHMe_2). $^{13}\text{C}\{^1\text{H}\}$ NMR [100.63 MHz, CDCl_3 , δ_{C} , ppm]: 167.1 (C^8), 154.7 (meade- C^6), 154.2 (meade- C^2), 151.7 (C^2), 150.2 (meade- C^4), 144.1 (meade- C^8), 143.8 (C^{8a}), 139.2 (C^4), 130.3 (C^6), 130.0 (C^{4a}), 124.3 (C^3), 117.2 (meade- C^5), 114.9 (C^7), 114.2 (C^5), 95.0 (cy- C^4), 91.9 (cy- C^1), 78.2, 76.2, 71.3, 71.1 (cy- $\text{C}^{2,3,5,6}$), 31.4 (CHMe_2), 30.5 (meade-Me), 23.3, 21.6 (CHMe_2), 17.8 (Me). NMR shifts and coupling constants for compounds **3b**, **6b**, **6c**, **7b**, and **7c** are quoted as Supporting Information.**

Crystallographic Structure Determination. X-ray diffraction measurements were performed on a Nonius Kappa CCD or Bruker X8 APEXII CCD diffractometer. Single crystals were positioned at 30, 40, 30, 30, 40, and 40 mm from the detector, and 502, 3001, 344, 344, 1145, and 5036 frames were measured, each for 40, 5, 40, 35, 2, and 10 s over 1.5, 1, 2, 2, 1, and 0.5° scan width for **4a**, **5b**, **6a**, **7a**, **7c**, and **9b**, correspondingly. The data were processed using Denzo-SMN or SAINT software.²¹ Crystal data, data collection parameters, and structure refinement details are given in Tables 1 and 2. The structures were solved by direct methods and refined by full-matrix least-squares techniques. Non-H atoms were refined with anisotropic displacement parameters. H atoms were inserted in calculated positions and refined with a riding model. The following computer programs were used: structure solution, SHELXS-97;²² refinement, SHELXL-97;²³ molecular diagrams, ORTEP;²⁴ computer, Pentium IV; scattering factors.²⁵

Table 1. Crystal Data and Details of Data Collection for **4a** · CH₂Cl₂, **5b** · 3CH₃OH, and **6a**

	4a · CH ₂ Cl ₂	5b · 3CH ₃ OH	6a
chemical formula	C ₂₈ H ₂₈ Cl ₂ F ₃ N ₃ O ₄ RuS	C ₂₉ H ₃₇ N ₃ O ₄ Os	C ₂₃ H ₂₄ F ₃ N ₃ O ₄ RuS
fw	731.56	681.82	596.58
space group	<i>P2₁/n</i>	<i>P1</i>	<i>P2₁/c</i>
<i>a</i> , Å	13.531(3)	10.4410(5)	12.819(3)
<i>b</i> , Å	11.219(2)	11.3821(5)	12.076(2)
<i>c</i> , Å	20.357(4)	13.4172(7)	15.823(3)
α , deg		90.499(3)	
β , deg	106.48(3)	108.143(2)	105.74(3)
γ , deg		112.641(2)	
<i>V</i> , Å ³	2963.3(10)	1383.35(12)	2357.6(8)
<i>Z</i>	4	2	4
λ , Å	0.71073	0.71073	0.71073
ρ_{calcd} , g cm ⁻³	1.640	1.637	1.681
cryst size, mm ³	0.40 × 0.29 × 0.04	0.34 × 0.32 × 0.23 × 0.20 × 0.32	0.14
<i>T</i> , K	120	100	120
μ , cm ⁻¹	8.38	46.47	8.14
R1 ^a	0.0273	0.0123	0.0227
wR2 ^b	0.0688	0.0304	0.0606
GOF ^c	1.044	1.065	1.099

^a R1 = $\sum|F_o| - |F_c|/\sum|F_o|$. ^b wR2 = $\{\sum[w(F_o^2 - F_c^2)^2]/\sum[w(F_o^2)^2]\}^{1/2}$. ^c GOF = $\{\sum[w(F_o^2 - F_c^2)^2]/(n - p)\}^{1/2}$, where *n* is the number of reflections and *p* is the total number of parameters refined.

Table 2. Crystal Data and Details of Data Collection for **7a** · 0.5(C₂H₅)₂O, **7c** · 2CH₃OH, and **9b**

	7a · 0.5(C ₂ H ₅) ₂ O	7c · 2CH ₃ OH	9b
chemical formula	C ₂₉ H ₃₁ F ₃ N ₃ O _{4.5} RuS	C ₂₈ H ₂₄ F ₆ N ₃ O ₃ OsP	C ₂₅ H ₂₇ F ₆ N ₆ O ₈ OsP
fw	683.70	795.75	762.70
space group	<i>C2/c</i>	<i>P1</i>	<i>P2₁/c</i>
<i>a</i> , Å	19.878(4)	9.2497(18)	17.261(4)
<i>b</i> , Å	22.441(4)	10.955(2)	10.044(2)
<i>c</i> , Å	14.179(3)	14.715(3)	16.238(3)
α , deg		77.78(3)	
β , deg	115.89(3)	87.82(3)	103.90(3)
γ , deg		83.83(3)	
<i>V</i> , Å ³	5690.2(19)	1448.7(5)	2732.7(9)
<i>Z</i>	8	2	4
λ , Å	0.71073	0.71073	0.71073
ρ_{calcd} , g cm ⁻³	1.596	1.824	1.854
cryst size, mm ³	0.28 × 0.17 × 0.11	0.50 × 0.40 × 0.18	0.15 × 0.15 × 0.03
<i>T</i> , K	120	100	296
μ , cm ⁻¹	6.87	45.31	47.97
R1 ^a	0.0308	0.0215	0.0279
wR2 ^b	0.0779	0.0525	0.0705
GOF ^c	1.061	1.030	1.047

^a R1 = $\sum|F_o| - |F_c|/\sum|F_o|$. ^b wR2 = $\{\sum[w(F_o^2 - F_c^2)^2]/\sum[w(F_o^2)^2]\}^{1/2}$. ^c GOF = $\{\sum[w(F_o^2 - F_c^2)^2]/(n - p)\}^{1/2}$, where *n* is the number of reflections and *p* is the total number of parameters refined.

Determination of Octanol/Water Partition Coefficients. The log *P* values were determined using the shake flask method. Both octanol and water were presaturated with water or octanol, respectively. Due to the low stability of the compounds in water/octanol mixture, the standard procedure was modified as follows: The sample compound was shaken intensively in a mixture of water and octanol for 2 h. Phase separation was achieved using a centrifuge (Sorvall, RT6000B) at 20 °C for 5 min at 3000 rpm. The compounds in the organic phase were quantified by using an UV–vis spectrophotometer (Perkin-Elmer, Lambda 7).

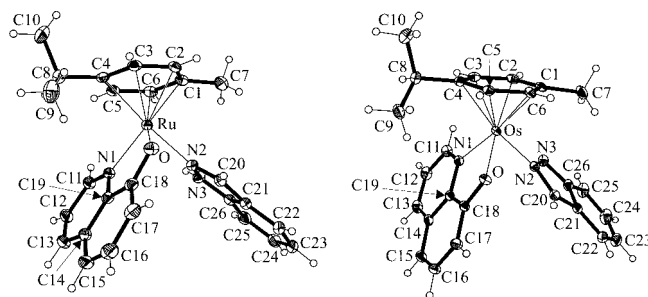
Cell Lines and Culture Conditions. CH1 cells (ovarian carcinoma) were kindly donated by Lloyd R. Kelland, CRC Centre

(22) Sheldrick, G. M. *SHELXS-97, Program for Crystal Structure Solution*; Göttingen: Germany, 1997.

(23) Sheldrick, G. M. *SHELXL-97, Program for Crystal Structure Refinement*; Göttingen, Germany, 1997.

(24) Johnson, G. K. *Report ORNL-5138*; Oak Ridge National Laboratory: Oak Ridge, TN, 1976.

(25) *International Tables for X-ray Crystallography*; Kluwer Academic Press: Dordrecht, The Netherlands, 1992; Vol. C, Tables 4.2.6.8 and 6.1.1.

**Figure 1.** Structure of the complex cation in **4a** (left) and of the complex **5b** (right).

for Cancer Therapeutics, Institute of Cancer Research, Sutton, UK. SW480 cells (adenocarcinoma of the colon) were kindly provided by Brigitte Marian, Institute of Cancer Research, Department of Medicine I, Medical University of Vienna, Austria. Cells were grown in 75 cm² culture flasks (Iwaki) as adherent monolayer cultures in complete culture medium, i.e., Minimal Essential Medium (MEM) supplemented with 1 mM sodium pyruvate, 4 mM L-glutamine, and 1% nonessential amino acids (100×) (all purchased from Sigma Aldrich) and 10% heat-inactivated fetal bovine serum (purchased from Gibco/Invitrogen). Cultures were maintained at 37 °C in a humidified atmosphere containing 5% CO₂.

Antiproliferative Activity in Cancer Cell Lines. Antiproliferative activity was determined by means of a colorimetric microculture assay (MTT assay, MTT = 3-(4,5-dimethyl-2-thiazolyl)-2,5-diphenyl-2H-tetrazolium bromide, purchased from Fluka). For this purpose, CH1 and SW480 cells were harvested from culture flasks by trypsinization and seeded in 100 μ L aliquots into 96-well microculture plates (Iwaki). Cell densities of 1.5×10^3 cells/well (CH1) and 2.5×10^3 cells/well (SW480) were chosen in order to ensure exponential growth throughout drug exposure. Cells were allowed to settle in drug-free complete culture medium for 24 h, followed by the addition of dilutions of the test compounds in 100 μ L/well complete culture medium and incubation for 96 h. At the end of exposure, drug solutions were replaced by 100 μ L/well RPMI1640 culture medium (supplemented with 10% heat-inactivated fetal bovine serum) plus 20 μ L/well MTT solution in phosphate-buffered saline (5 mg/ml PBS). After incubation for 4 h, the medium/MTT mixtures were removed, and the formazan product formed by vital cells was dissolved in 150 μ L of DMSO per well. Optical densities at 550 nm were measured with a microplate reader (Tecan Spectra Classic), using a reference wavelength of 690 nm to correct for unspecific absorption. The quantity of vital cells was expressed in terms of T/C values by comparison to untreated control microcultures, and IC₅₀ values were calculated from concentration–effect curves by interpolation. Evaluation is based on means from at least three independent experiments, each comprising six replicates per concentration level.

Results and Discussion

Synthesis. The reaction of $[(\eta^6\text{-}p\text{-cymene})\text{RuCl}_2]_2$ with 2 equiv of K(oxine) in ice-cold CH₂Cl₂ afforded the half-sandwich complex **1a** in 92% yield. The spectroscopic properties of **1a** were identical with those of $[(\eta^6\text{-}p\text{-cymene})\text{Ru}(\text{oxine})\text{Cl}]$ prepared by using THF as a solvent.¹⁹ Compound **1b** was obtained by reaction of 8-hydroxyquinoline with sodium methoxide and $[(\eta^6\text{-}p\text{-cymene})\text{OsCl}_2]_2$ in approximately 2:2:1 molar ratio in methanol in 84% yield.²⁰ The monoqua complexes **2a** and **2b** were generated *in situ* by treatment of complexes **1a** and **1b** with equivalent amounts of AgNO₃ in water. The ¹H NMR spectra, which are similar to those of the starting compounds, indicate that the complexes are rather stable in aqueous solution.

Compounds **3a**, **4a**, **6a**, and **7a** were synthesized in 67, 65, 68, and 75% yield, correspondingly, starting from equivalent

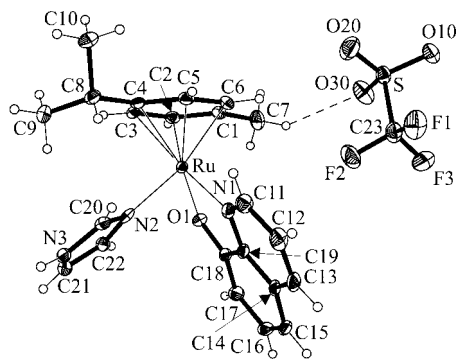


Figure 2. Structure of the ion pair in **6a**.

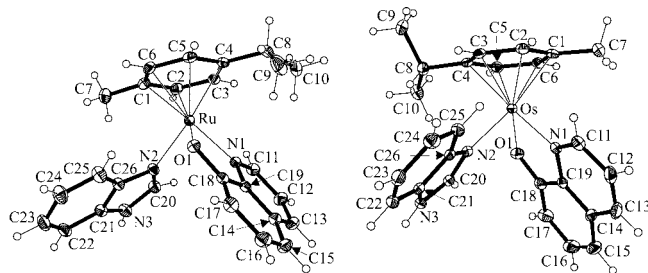


Figure 3. Structure of the complex cation in **7a** · 0.5(C₂H₅)₂O (left) and in **7c** (right).

Table 3. Selected Bond Distances (Å) and Angles (deg) for Complexes **4a**, **5a**, **5c**, **6a**, and **7b**

	4a	5a	5c	6a	7b
M–O1	2.0853(14)	2.0771(15)	2.069(2)	2.0664(12)	2.0678(9)
M–N1	2.0911(16)	2.0926(14)	2.069(2)	2.0664(12)	2.0678(9)
M–N2	2.0950(17)	2.1027(14)	2.131(3)	2.1107(13)	2.0899(12)
M–C(1–6) _{av}	2.198(7)	2.196(9)	2.190(7)	2.192(8)	2.188(9)
C–C(1–6) _{av}	1.422(6)	1.419(3)	1.421(4)	1.417(3)	1.424(2)
O1–M–N1	78.55(6)	78.71(5)	78.83(10)	79.11(5)	78.34(4)
O1–M–N2	83.17(6)	86.22(5)	81.28(10)	83.01(5)	82.81(4)
N1–M–N2	85.08(6)	83.33(6)	83.89(10)	85.73(5)	82.46(4)

amounts of **1a** and AgCF₃SO₃ in THF to which the corresponding azole ligand was added. The synthesis of osmium compounds **3b**, **6b**, and **7b** was performed similarly in 61, 62, and 69% yield, respectively, by using methanol instead of THF as a solvent. The noncharged species **5b** with a deprotonated indazole ligand was obtained in 43% yield by reacting **1b** with Ag₂CO₃ and indazole in 2:1:2 molar ratio in methanol. The chloride salt **6c** was synthesized from equivalent amounts of **1b** and imidazole in methanol at room temperature in 83% yield, while the hexafluorophosphate salt **7c** was obtained by reaction of **1b** with AgPF₆ in 1:1 molar ratio, followed by addition of the equivalent quantity of benzimidazole at room temperature, in 72% yield. When the mixture of **1b** with 9-methyladenine was allowed to react in methanol for 1 h and then added to an aqueous solution of NH₄PF₆, the complex **9b** was obtained. Recrystallization of the latter from methanol saturated with diethyl ether afforded large yellow-brown crystals of the pure compound in 47% yield.

Crystal Structures. We determined the X-ray diffraction structures of [(η⁶-*p*-cymene)Ru(oxine)(Hind)]CF₃SO₃ · CH₂Cl₂ (**4a** · CH₂Cl₂), [(η⁶-*p*-cymene)Os(oxine)(ind)] · 3CH₃OH (**5b** · 3CH₃OH, Figure 1), [(η⁶-*p*-cymene)Ru(oxine)(Him)] · CF₃SO₃ (**6a**, Figure 2), [(η⁶-*p*-cymene)Ru(oxine)(Hbzim)] · CF₃SO₃ · 0.5(C₂H₅)₂O (**7a** · 0.5(C₂H₅)₂O), and [(η⁶-*p*-cymene)Os(oxine)(Hbzim)]PF₆ · 2CH₃OH (**7c** · 2CH₃OH, Figure 3). All complexes have the characteristic “three-leg piano-stool” geometry of Ru(II) or Os(II) arene complexes, with an η⁶ π-bound

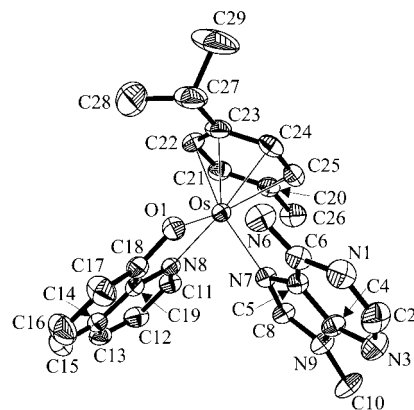


Figure 4. Structure of the complex cation in **9b**. Selected bond distances (Å): Os–O1 2.076(3), Os–N7 2.124(3), Os–N8 2.089(3), Os–C(1–6)_{av} 2.187(9).

p-cymene ring forming the seat and three other donor atoms of one bidentate oxine ligand and one azole ligand as the legs of the stool. They are racemates due to the presence of the stereogenic metal center. Selected bond distances and angles are quoted in Table 3. The X-ray structure of complex **7c** · 2CH₃OH (Figure 3) is the first of a monoarene complex of osmium, in which an oxine and an azole ligand are bound to the same metal center, while that of compound **5b** · 3CH₃OH is the first of a monoarene complex of osmium with a deprotonated azole ligand.

A large number of transition metal complexes with pyrazoles and/or pyrazolates have been documented in the literature.^{26–28} Coordinated pyrazole ligands are either protonated or deprotonated, depending on reaction conditions and the metal ion identity.²⁹ The proton in coordinated pyrazole is often involved in hydrogen bonding.³⁰ The deprotonated pyrazole normally acts as a bridging ligand, enabling the formation of dinuclear³¹ or cyclic polynuclear complexes.^{29,32} In contrast, indazole acts mainly as a monodentate protonated ligand in metal complexes. In a few cases, it was found to be deprotonated, acting as a bridging ligand in polynuclear metal complexes³³ or even more rarely as a monodentate indazolate ligand.³⁴

[(η⁶-*p*-cymene)Os(oxine)(meade)]PF₆ (**9b**) crystallized in the monoclinic space group *P*2₁/*c*. The structure of the complex cation is shown in Figure 4. A part of the crystal structure of **9b**, displaying the coordinated 9-methyladenine (meade) pairing via intermolecular hydrogen bonding interactions, is shown in Figure S1. Selected bond distances (Å) and angles (deg) are quoted in the legends to Figures 4 and S1. The 9-methyladenine ligand is coordinated to osmium through nitrogen atom N7 in

(26) Trofimenko, S. *Prog. Inorg. Chem.* **1986**, *34*, 115–210.

(27) Sadimenko, A. P. *Adv. Heterocycl. Chem.* **2001**, *80*, 157–240.

(28) La Monica, G.; Ardizzone, G. A. *Prog. Inorg. Chem.* **1997**, *46*, 151–238.

(29) Umakoshi, K.; Yamauchi, Y.; Nakamiya, K.; Kojima, T.; Yamasaki, M.; Kawano, S. H.; Onishi, M. *Inorg. Chem.* **2003**, *42*, 3907–3916.

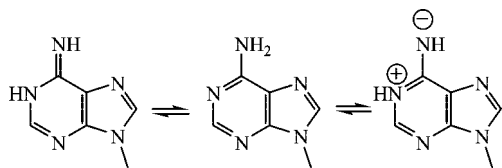
(30) Stepanenko, I. N.; Cebrian-Losantos, B.; Arion, V. B.; Krokhin, A.; Nazarov, A. A.; Keppler, B. K. *Eur. J. Inorg. Chem.* **2007**, 400–411.

(31) (a) Beveridge, K. A.; Bushnell, G. W.; Dixon, K. R.; Eadie, D. T.; Stobart, S. R.; Atwood, J. L.; Zaworotko, M. J. *J. Am. Chem. Soc.* **1982**, *104*, 920–922. (b) Coleman, A. W.; Eadie, D. T.; Stobart, S. R.; Zaworotko, M. J.; Atwood, J. L. *J. Am. Chem. Soc.* **1982**, *104*, 922–923.

(32) Burger, W.; Strähle, J. Z. *Anorg. Allg. Chem.* **1985**, *529*, 111–117.

(33) (a) Rendle, D. F.; Storr, A.; Trotter, J. *Can. J. Chem.* **1975**, *53*, 2930–2943. (b) Cortes-Llamas, S. A.; Hernández-Pérez, J. M.; Hô, M.; Muñoz-Hernández, M.-A. *Organometallics* **2006**, *25*, 588–595.

(34) Fackler, J. P., Jr.; Staples, R. J.; Raptis, R. G. Z. *Kristallogr.* **1997**, *212*, 157–158.

Chart 2. Tautomeric Structures of 9-Methyladenine: the Imine Form (left), the Amine Form (middle), and the Zwitterionic Form (right)

its amine form (Chart 2). The Os–N7 bond (see legend to Figure 4) is longer than that in $[(\eta^6\text{-}p\text{-cymene})\text{Os}(\text{pico})(9\text{EtA})]\text{PF}_6 \cdot 0.5\text{Et}_2\text{O}$ at 150 K [2.094(7) Å], where pico = picolate.²⁰ Coordination of 9-substituted adenine via the ring nitrogen atoms is governed first of all by their basicity, which decreases in the order N1 > N7 > N3. In some cases, metal ions can also bind to the exocyclic amine group with concomitant loss of one proton or its migration to the neighboring ring nitrogen atom N1 and stabilization of the rare imine tautomer (Chart 2).³⁵ Bridging and/or chelate interactions involving different combinations of exocyclic and endocyclic nitrogen atoms and even the C8 of the imidazole ring have also been demonstrated by X-ray diffraction.³⁶ This is to our knowledge the second crystallographic evidence for a monodentate coordination mode of 9-alkyladenine to osmium documented so far.³⁷ The amine group of 9-methyladenine in **9b** acts as a hydrogen donor and N1 as a hydrogen acceptor, which are involved in complex pairing through strong intermolecular hydrogen bonding as shown in Figure S1. Similar purine base pairing was observed for $[(\eta^6\text{-}p\text{-cymene})\text{Os}(\text{pico})(9\text{EtA})]\text{PF}_6 \cdot 0.5\text{Et}_2\text{O}$ ²⁰ and $[\text{Ru}^{\text{III}}\text{Cl}_3\text{-(Hind)}_2(\text{meade})] \cdot \text{CH}_2\text{Cl}_2 \cdot \text{CH}_3\text{OH}$ or $[\text{Ru}^{\text{III}}\text{Cl}_3(\text{Hind})_2(\text{meade})] \cdot 1.1\text{H}_2\text{O} \cdot 0.9\text{CH}_3\text{OH}$.³⁸ The same amine group of 9-methyladenine and the oxygen atom of the oxine ligand O1 are involved in intramolecular hydrogen bonding (see Figure S1).

Aqueous Solubility, Lipophilicity, and Hydrolytic Stability. The aqueous solubility of the family of complexes prepared varies from 0.3 mM (**7b**) to 52.3 mM (**6c**). This depends on the metal ion, the identity of the azole heterocycle, and the counteranion. Generally, the ruthenium complexes isolated are more soluble in water than their osmium(II) congeners. The effect of the azole heterocycle on the aqueous solubility of the complexes is different, as anticipated from comparison of their lipophilicity, expressed by the octanol–water partitioning coefficients ($\log P_{\text{o/w}}$) for imidazole (−0.08),³⁹ pyrazole (0.13),⁴⁰ benzimidazole (1.32⁴¹ or 1.38⁴²), indazole (1.77),³⁹ and 5,6-

Table 4. Maximum Absorption Wavelength and $\log P_{\text{o/w}}$ Values for Compounds **3a, **6b**, and **7a****

complex	λ_{max} (nm)	$\log P_{\text{o/w}}$
3a	399	0.98 ± 0.02
6b	431	1.18 ± 0.01
7a	405	1.79 ± 0.08

dimethylbenzimidazole (2.35).⁴¹ Chlorides show the highest aqueous solubility when compared to triflates and hexafluorophosphates. We also succeeded in determining the $\log P_{\text{o/w}}$ values for ruthenium and osmium complexes **3a**, **6b**, and **7a** by UV–vis spectroscopy, using the shake–flask method.⁴³ The partition of ions between octanol and aqueous phase is a more complex process than that of neutral species. The observed concentration ratio for the complex cation $[(\eta^6\text{-}p\text{-cymene})\text{Ru}(\text{oxine})(\text{Hazole})]^+$ is related not only to the partition of the cation but also to the partition of the ion pair.⁴⁴ Nevertheless, we believe that the data obtained (Table 4) can be used for relative estimation of lipophilicity, since the concentration ratio $[\text{C}]_{\text{o}}/[\text{C}]_{\text{w}}$ was obtained at very low concentrations of solute, so that the presence of only single ions is likely. Moreover, the $\log P_{\text{o/w}}$ value for compound **3a** was found to be independent of solute concentration. It should, however, be noted that the determination of $\log P_{\text{o/w}}$ values of the other compounds was precluded by the observed slow decomposition of compounds, evidenced by the appearance of a green color, upon shaking the octanol/water mixture of compounds and separation of octanol and aqueous phases, which requires prolonged times. UV–vis spectra for complex **6a** showing its degradation during the measurement are given in the Supporting Information. The differences in the spectra are similar to those of **3b**, **6c**, and **4a**, which undergo transformation as well. To reduce the time-dependent effect of the octanol/water mixture on the decomposition of compounds **3a**, **6b**, and **7a**, the separation of liquid phases was accelerated by using centrifugation. As expected, the lipophilicity of these complexes (Table 4) is mainly determined by the lipophilicity of the ancillary azole ligands.

The hydrolytic stability of osmium complexes **3b**, **6b**, and **6c** in D₂O was studied by ¹H NMR spectroscopy. The ¹H NMR spectra measured immediately and 96 h after dissolution at room temperature were almost identical (Figures S1–S3), indicating that they maintain their structural integrity in solution. The stability of **6c** in water and **7a** in *n*-octanol was also confirmed by electronic absorption spectra, which were recorded immediately and 24 h after dissolution at room temperature with no change in the spectra. The ESI mass spectra of the solution of **6c** after 96 h showed a peak at *m/z* 447, attributed to the intact complex cation $[(\eta^6\text{-}p\text{-cymene})\text{Os}(\text{oxine})(\text{Him})]^+$.

Antiproliferative Activity. The ability of six ruthenium-based (**1a**, **2a**, **3a**, **4a**, **6a**, **7a**) complexes and their osmium-based (**1b**, **2b**, **3b**, **6b**, **6c**) analogues to inhibit cancer cell proliferation *in vitro* was investigated in the human cell lines CH1 (ovarian carcinoma) and SW480 (colon carcinoma) by means of the MTT assay with 96 h exposure. Concentration–effect curves are depicted in Figure 5, and IC₅₀ values are listed in Table 5.

In general, the investigated complexes show respectable antiproliferative activity in low micromolar concentrations in both cell lines. SW480 colon carcinoma cells are slightly (up to 2.1 times, based on comparison of IC₅₀ values) more sensitive than CH1 ovarian carcinoma cells to the ruthenium compounds, with the single exception of the pyrazole complex **3a**. Differences between sensitivities to the osmium complexes are mostly

(35) (a) Kuo, L. Y.; Kanatzidis, M. G.; Sabat, M.; Tipton, A. L.; Marks, T. J. *J. Am. Chem. Soc.* **1991**, *113*, 9027–9045. (b) Zamora, F.; Kunsman, M.; Sabat, M.; Lippert, B. *Inorg. Chem.* **1997**, *36*, 1583–1587. (c) Clarke, M. J. *J. Am. Chem. Soc.* **1978**, *100*, 5068–5075. (d) Arpalahiti, J.; Klika, K. D. *Eur. J. Inorg. Chem.* **1999**, *8*, 1199–1201. (e) Viljanen, J.; Klika, K. D.; Sillampää, R.; Arpalahiti, J. *Inorg. Chem.* **1999**, *38*, 4924–4925.

(36) (a) Trovó, G.; Bandoli, G.; Nicolini, M.; Longato, B. *Inorg. Chim. Acta* **1993**, *211*, 95–99. (b) Olivier, M. J.; Beauchamp, A. L. *Acta Crystallogr.* **1982**, *B38*, 2159–2162. (c) Prizant, L.; Olivier, M. J.; Rivest, R.; Beauchamp, A. L. *J. Am. Chem. Soc.* **1979**, *101*, 2765–2767.

(37) CSD version 5.29; November 2007.

(38) Egger, A.; Arion, V. B.; Reiser, E.; Cebrián-Losantos, B.; Shova, S.; Trettenhahn, G.; Keppler, B. K. *Inorg. Chem.* **2005**, *44*, 122–132.

(39) Kibbey, C. E.; Poole, S. K.; Robinson, B.; Jackson, J. D.; Durham, D. *J. Pharm. Sci.* **2001**, *90*, 1164–1175.

(40) (a) Chou, J. T.; Jurs, P. C. In *Solubility and Partitioning in Drug Design: Physical Chemical Properties of Drug*; Yalkowsky, S. H., Sinkula, A. A., Valvani, C. C., Eds.; Marcel Dekker: New York, 1980; pp 163–199. (b) Bodor, N.; Hung, M. J. *J. Pharm. Sci.* **1992**, *81*, 272–281.

(41) Mannhold, R.; Cruciani, G.; Dross, K.; Rekker, R. *J. Comput.-Aided Mol. Des.* **1998**, *12*, 573–581.

(42) Bodor, N.; Gabanyi, Z.; Wong, C.-K. *J. Am. Chem. Soc.* **1989**, *111*, 3783–3786.

(43) Qiao, Y.; Xia, S.; Ma, P. *J. Chem. Eng. Data* **2008**, *53*, 280–282.

(44) Zhao, Y. H.; Abraham, M. H. *J. Org. Chem.* **2005**, *70*, 2633–2640.

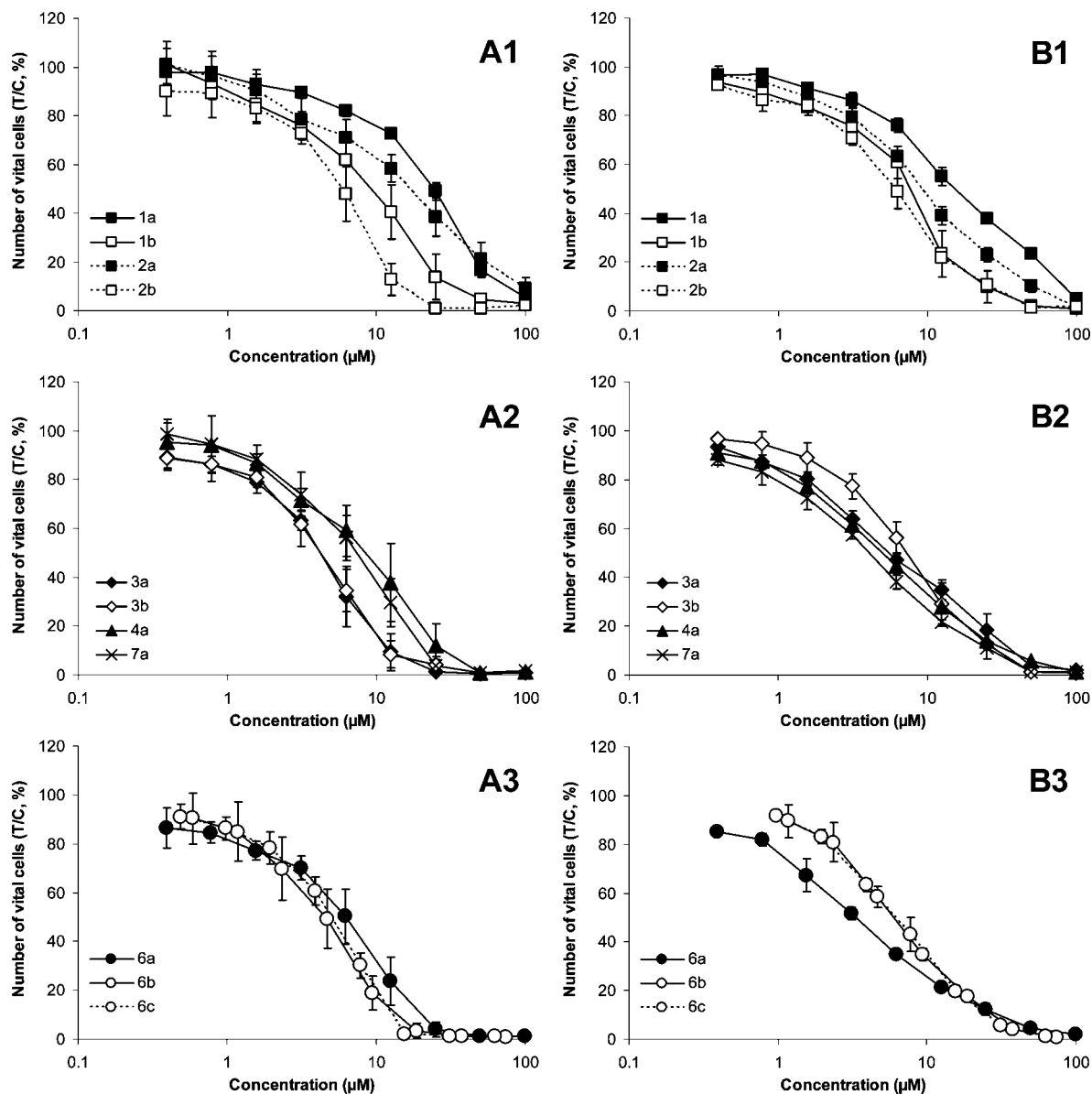


Figure 5. Concentration–effect curves of the compounds in two human cancer cell lines (A1–3: CH1; B1–3: SW480).

Table 5. Antiproliferative Activity of Ruthenium Complexes (**1a**, **2a**, **3a**, **4a**, **6a**, and **7a**) and Osmium Complexes (**1b**, **2b**, **3b**, **6b**, and **6c**) in Two Human Cancer Cell Lines

compound	IC_{50} (μM) ^a	
	CH1	SW480
1a	24.2 ± 2.0	15.3 ± 2.1
1b	9.7 ± 1.8	7.7 ± 1.1
2a	17.0 ± 3.7	9.2 ± 0.9
2b	6.1 ± 1.3	6.0 ± 1.0
3a	5.5 ± 1.2	7.6 ± 1.9
3b	4.3 ± 0.9	7.5 ± 1.3
4a	9.4 ± 3.0	5.2 ± 0.8
6a	7.0 ± 2.7	3.3 ± 0.4
6b	4.5 ± 1.5	6.0 ± 0.6
6c	5.0 ± 0.6	6.5 ± 1.3
7a	7.4 ± 1.9	4.1 ± 0.2

^a 50% inhibitory concentrations after exposure for 96 h in the MTT assay. Values are means ± standard deviations, obtained from at least three independent experiments.

less pronounced and within the ranges of variation, except for the pyrazole complex **3b**, which behaves similarly to **3a**.

Since it is difficult to isolate mono-aqua species in the solid state, compounds **2a** and **2b** were generated *in situ* as described

in the Experimental Section. A comparison of the concentration–effect curves of the chlorido complexes (**1a**, **1b**) with their activated counterparts (**2a**, **2b**) (Figure 5, parts A1, B1) reveals that the activated species show a higher antiproliferative activity in both cases, in accordance with the expectation that forced complete hydrolysis results in increased reactivity of the complexes. Furthermore, the osmium species **1b** and **2b** are 2.5–2.8 times (CH1) and 1.5–2.0 times (SW480) more active than the ruthenium congeners **1a** and **2a**, based on comparison of IC_{50} values.

As can be seen in Figure 5, parts A2 and B2, all three complexes with an imidazole ligand exert similar effects. The change of the metal center from ruthenium (**6a**) to osmium (**6b**) has a smaller impact than in the compounds mentioned above, and the change of the counteranion of the complex $[(\eta^6\text{-}p\text{-cymene})\text{Os}(\text{oxine})(\text{Him})]^+$ from triflate (**6b**) to chloride (**6c**) does not result in any meaningful differences. Likewise, the ruthenium (**3a**) and osmium (**3b**) complexes with a pyrazole ligand have similar activity (Figure 5, parts A3, B3). Variation of the azole ligand, e.g., indazole (**4a**) or benzimidazole (**7a**), results only in minor differences of antiproliferative activity,

and no conclusive structure–activity relationships can be deduced in this respect. Although a higher lipophilicity of the azole ligand might favor cellular uptake and thereby biological activity of the complex, no correlation can be found, neither between IC_{50} values of the complexes and $\log P$ values of the azole ligands (as reported in the literature cited in the previous section) nor between IC_{50} values and $\log P$ values or aqueous solubility of the complexes.

Within the ruthenium series, complexes containing a monodentate azole ligand show a 2.6–4.4 times (CH1) and 2.0–4.6 times (SW480) higher antiproliferative activity than the chlorido analogue **1a**, based on comparison of IC_{50} values. Their activity even exceeds that of the aqua analogue **2a**, although the less easily exchangeable azole ligands should be less favorable for coordination to target molecules. Within the osmium series, differences are much less pronounced, and no consistent structure–activity relationships are discernible.⁴⁴

Conclusions

We reported the synthesis of ruthenium(II) and osmium(II) arene complexes that combine ligands involved in metal-based complexes that are currently in clinical development, namely, oxine, which acts as a ligand in Ga(oxine)₃ (KP46), as well as azole ligands, which play a role in *trans*-[Ru^{III}Cl₄(Hind)₂][−] (KP1019) and *trans*-[Ru^{III}Cl₄(Him)(DMSO)][−] (NAMI-A). The aqueous solubility of the complexes reported in this study varies from 0.3 mM (**7b**) to 53.3 mM (**6c**) and depends on the metal ion, the identity of the azole heterocycle, and the counteranion.

The osmium complexes are slightly less soluble in water than the corresponding ruthenium compounds. The lipophilicity of organometallic compounds, expressed by octanol/water partition coefficients, can be to some extent controlled by the azole heterocycle used as co-ligand. Both ruthenium and osmium arene complexes with oxine and an azole heterocycle as ancillary ligands are highly cytotoxic in the human tumor cell lines SW480 (colon carcinoma) and CH1 (ovarian carcinoma), with IC_{50} values ranging from 3.3 to 9.4 μ M, and should therefore be considered as potential novel anticancer drugs.

Acknowledgment. We thank A. Roller for the collection of X-ray data sets and Prof. M. Galanski for the measurement of NMR spectra.

Supporting Information Available: Crystallographic data for **4a** · CH₂Cl₂, **5b** · 3CH₃OH, **6a**, **7a** · 0.5(C₂H₅)₂O, **7c** · 2CH₃OH, and **9b** in CIF format, details of crystal structure of **9b** showing the coordinated 9-methyladenine pairing via intermolecular H-bonding interactions (Figure S1), time-independent ¹H NMR spectra of compounds **3b**, **6b**, and **6c** in D₂O (Figures S2–S4), time-independent UV–vis spectra of compounds **3a**, **4a**, **6a**, and **7a** in water (Figures S5–S7, S9), time-independent UV–vis spectra of **7a** in *n*-octanol (Figure S10), and UV–vis spectra of **6a** in *n*-octanol, measured immediately after dissolution and after 2 h of shaking with water followed by phase separation (Figure S8). This material is available free of charge via the Internet at <http://pubs.acs.org>.

OM800774T